

Information Criteria for quantifying loss of reversibility in parallelized KMC

Konstantinos Gourgoulis^{a,*}, Markos A. Katsoulakis^a, Luc Rey-Bellet^a

^a*Department of Mathematics and Statistics, Lederle Graduate Research Tower, University of Massachusetts, 710 N. Pleasant Street, Amherst, MA, 01003-9305*

Abstract

Parallel Kinetic Monte Carlo (KMC) is a potent tool to simulate stochastic particle systems efficiently. However, despite literature on quantifying domain decomposition errors of the particle system for this class of algorithms in the short and in the long time regime, no study yet explores and quantifies the loss of time-reversibility in Parallel KMC. Inspired by concepts from non-equilibrium statistical mechanics, we propose the entropy production per unit time, or entropy production rate, given in terms of an observable and a corresponding estimator, as a metric that quantifies the loss of reversibility. Typically, this is a quantity that cannot be computed explicitly for Parallel KMC, which is why we develop *a posteriori* estimators that have good scaling properties with respect to the size of the system. Through these estimators, we can connect the different parameters of the scheme, such as the communication time step of the parallelization, the choice of the domain decomposition, and the computational schedule, with its performance in controlling the loss of reversibility. From this point of view, the entropy production rate can be seen both as an information criterion to compare the reversibility of different parallel schemes and as a tool to diagnose reversibility issues with a particular scheme. As demonstration, we use Sandia Lab's SPPARKS software to compare different parallelization schemes and different domain (lattice) decompositions.

Keywords: parallel kinetic Monte Carlo, operator splitting schemes, long-time errors, time-reversibility, detailed balance, entropy production, information criteria

1. Introduction

Kinetic Monte Carlo, also known as the n-fold way [1] or the Bortz-Kalos-Lebowitz algorithm [2], is a common tool among practitioners interested in simulating stochastic processes arising from chemical, biological, or agent-based

*Corresponding author. e-mail: gourgoul@math.umass.edu

models on lattices [3]. However, even sophisticated algorithms inevitably experience slowdown as the size of the system increases. In fact, it may even be the case that the system size prohibits the use of a serial simulation, for instance due to problems with storing the system in a single CPU's memory.

There is a substantial amount of work in addressing the efficiency issues when simulating larger time and length scales by using parallel algorithms for systems with either short-range [4, 5, 6] or long-range interactions [7, 8]. Typically, those algorithms are based on domain decomposition of the lattice into sub-domains (see Figure 1), and subsequently the simulation on each sub-domain according to a chosen computational schedule. One such algorithm is part of Sandia Labs' SPPARKS Monte Carlo code [9]. A new insight from [10] was that such parallel KMC algorithms that depend on short-range interactions can be formulated as operator splitting schemes that approximate the exact process. This mathematical formulation allows both for performance and numerical error analysis of the schemes [11]. It was also leveraged in previous work [12] where, combined with information metrics, allowed us to study the long time error behavior of the schemes.

In fact, the investigation of long-time errors for operator splitting schemes is of prime importance when using parallel KMC, as errors accumulate due to the domain decomposition procedure. This accumulation can affect the simulation dramatically at long times and make it hard or uncertain for practitioners to sample from the correct stationary regime. Unfortunately, classical numerical analysis fails to quantify errors of splitting schemes, such as parallel KMC, for long times, which in turn motivated our use of the relative entropy per unit time as a tool to study the performance of operator splitting schemes [12].

The other aspect of long-time behavior, and the focus of this work, is on systems with time-reversible dynamics. That symmetry is often an integral part of the physical structure of the model, for example in the simulation of interacting diffusions or adsorption/desorption mechanisms. While in such cases the time-reversal symmetry is preserved under the serial KMC simulation (typically by enforcing the detailed balance condition), the time-discretization, domain decomposition, and breakdown of serial communication of the parallelized algorithm may lead to loss of detailed balance, and thus of reversibility. There exists some literature on constructing a synchronous parallel algorithm that partially preserves the detailed balance (DB) condition [13], but such schemes will not be considered in this work. Instead, our focus is on general partially asynchronous parallel algorithms, like the one in SPPARKS. For those, a user has to pick between different domain decompositions, time steps of the scheme, and the computational schedule. As expected, these choices will impact the loss of reversibility of the scheme. Therefore, it makes sense to develop a theory that can connect the various parameters of the scheme with loss of reversibility.

Regarding the loss of reversibility of numerical schemes, in [14] the authors used the entropy production rate (EPR) as an information metric to quantify the loss of reversibility for the Euler-Maruyama and Milstein schemes for stochastic differential equations, as well as BBK schemes for Langevin dynamics. This idea was motivated by concepts in non-equilibrium statistical mechanics, originally

developed to understand the long-time dynamics and the fluctuations in non-equilibrium steady states [15, 16, 17, 18, 19]. The authors in [14] used such non-equilibrium statistical mechanics methods as computable numerical tools to assess the loss of reversibility of numerical schemes for SDEs. More specifically, they computed the EPR with the Gallavotti-Cohen action functional [17] as an estimator for different numerical schemes. It was demonstrated that the scheme performance in controlling the loss of reversibility can vary greatly. In particular, the Euler-Maruyama scheme for SDEs with multiplicative noise can break reversibility in an unrecoverable manner regardless of the size of the time step [14, Theorem 3.7].

Our goal here is to apply a similar perspective for the study of splitting schemes in parallel KMC. However, in contrast with schemes for SDEs, for the class of systems that we can simulate in this manner the transition probabilities are either difficult to compute or not available at all. Because of this fact, a new approach is required, which is why we write the EPR as an asymptotic expansion in the scheme's time step by using the semigroup theory for Markov chains. We demonstrate that the coefficients of the expansion of the EPR depend on the transition rates of the model and can be estimated as ergodic averages by samples from the parallel algorithm. We also show that the required computations for the estimation of the coefficients scale with the size of the boundary between sub-domains on the lattice in a manner that depends on the scheme selected. Therefore, by appropriate normalization, we can calculate the entropy production rate per lattice site, i.e. independent of system size. As a result, we obtain an *a posteriori* expansion for the estimator of the EPR, which can be used as a diagnostic tool that can be calculated on a system of smaller size than the targeted one, and/or even ran with a simple serial implementation of the parallel algorithm.

This information-theoretical perspective is similar to the use of information metrics to assess discrepancy of models, algorithms, approximations, etc., to that applied to the study of long time errors for Parallel KMC [12], sensitivity analysis [20], and in studying loss of information due to coarse-graining in non-equilibrium systems [21].

The manuscript is organized as follows. In Section 2, we provide an introduction to Parallel Lattice KMC and the ideas behind its error analysis based on operator splitting. Section 3 is especially important, as we introduce the entropy production and entropy production per unit time. Those concepts will be the information-theoretical quantities used to study loss of reversibility for operator splitting schemes. Then, in Section 4, we discuss the estimation of the EPR, referring to specific examples and an implementation in SPPARKS. We use the estimates to compare two splitting schemes as well as discuss their loss of reversibility with respect to lattice decomposition and time step. Finally, in Section 5, we provide general results for the asymptotic behavior of EPR, and deduce from them estimators.

2. Background on Parallel Lattice KMC

Parallel Lattice KMC is an approximation to the exact, but serial, simulation algorithm. In implementations, it works by taking advantage of the spatial dependencies between the different events. For example, in a model with finite range interactions, the spins on two lattice sites can change with no error to the dynamics as long as the two are sufficiently far apart. Therefore, by decomposing the lattice into sub-lattices, we gain an efficient alternative to serial KMC analogous to domain decomposition methods in parallel algorithms for partial differential equations.

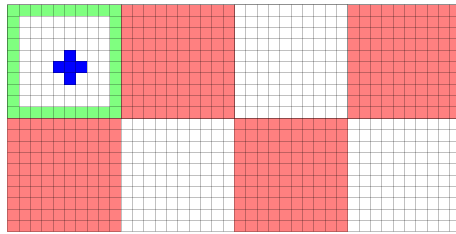


Figure 1: Checkerboard decomposition of a rectangular lattice into sub-lattices. Because each site's transition depends on the information from the **nearest neighbors**, transitions in sub-lattices of the same color are independent. White sub-lattices can be simulated asynchronously in time, while keeping the states in the red ones **frozen**. When the stochastic time reaches Δt , information is shared with the red sub-lattices about the state of the **boundary regions** (here only shown for the first sub-lattice).

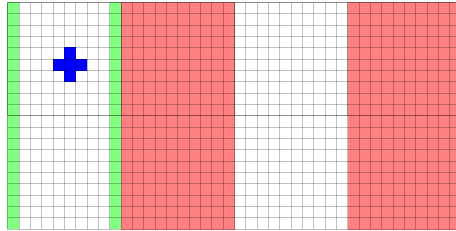


Figure 2: Stripe decomposition of a rectangular lattice into sub-lattices. Compared to Figure 1, now each processor needs to store more information before the runs can take place. However, the **boundary regions** (here only shown for the first sub-lattice) have shrunk, which leads to less error per time step [11, 12]. This can also be seen in Figure 3.

Nevertheless, as can be seen in Figure 1, for lattice sites in the boundary between domains, the transition rates will depend on the configurations in nearby

sub-domains, as well as the time window Δt during which sub-domains are kept frozen, see Figure 1. This communication procedure inevitably causes an accuracy penalty that the user needs to control, balancing the efficiency of the simulator with the error produced.

A new insight provided in [10] was the fact that parallel algorithms, such as the one described in Figure 1, can be formulated as operator splitting schemes. This connection allows for the design, error quantification, and performance analysis of such algorithms [11]. Specifically, this approach allows for an observable-focused error analysis, through which a practitioner can pick both the scheme class and specific parameters that fit the computational needs. Additionally, it formalizes the dependence of the error on the decomposition of the lattice and on the splitting time step, Δt , for bounded time intervals. Finally, it also allows to study the long-time behavior of the schemes and provides long-time error control in the recent work [12].

To begin, we pick a positive *operator splitting time step* Δt . If we were to simulate a Continuous Time Markov Chain via the serial KMC algorithm, then the corresponding transition probability of the process jumping from a state σ to a state σ' , $\sigma, \sigma' \in S$, in time t would be

$$P_t(\sigma, \sigma') = P(\sigma_t = \sigma' | \sigma_0 = \sigma) = e^{tL} \delta_{\sigma'}(\sigma). \quad (1)$$

In (1), $\delta_{\sigma'}$ is a Dirac probability measure, centered at state σ' and L is the generator of the process which, for bounded and continuous functions f , is defined as

$$L[f](\sigma) := \sum_{\sigma' \in S} q(\sigma, \sigma') (f(\sigma') - f(\sigma)). \quad (2)$$

Since the approximate process will be a discretization with Δt step size, we will be comparing it against the Δt -skeleton of the exact Continuous Time Markov Chain, with transition probability $P_{\Delta t}(\sigma, \sigma') = e^{\Delta t L} \delta_{\sigma'}(\sigma)$. Now, inspired by the Trotter product formula [22], one can write approximations to $e^{\Delta t L}$ by splitting the operator L into $L_1 + L_2$ (with associated rates q_1, q_2). For example, two popular approximations are:

$$e^{\Delta t L} \simeq e^{\Delta t L_1} e^{\Delta t L_2}, \quad (\text{Lie}) \quad (3)$$

$$e^{\Delta t L} \simeq e^{\Delta t/2 L_1} e^{\Delta t L_2} e^{\Delta t/2 L_1}. \quad (\text{Strang}) \quad (4)$$

Throughout this work, we shall be using $Q_{\Delta t}$ to denote the transition probability arising from approximations to $e^{\Delta t L}$. We will also use μ_Q to denote the corresponding stationary measure.

Practitioners are not limited to the operators L_1, L_2 . For example, the Sandia Lab's SPPARKS code [9] decomposes L into four pieces instead of two for 2D lattice simulations. However, the error analysis extends naturally to this case.

2.1. Local Error Analysis

One of the insights in [10] was that any operator splitting approximation is equivalent to a specific computational schedule for Parallel Lattice KMC. For example, if we alternate between the red and white groups in Figure 1, allowing each group to run only for Δt , then that is equivalent to using splitting (3) to approximate $e^{\Delta t L}$. If L is a bounded operator, then we can write the semigroup as a series expansion,

$$e^{\Delta t L} = \sum_{k=0}^{\infty} \frac{\Delta t^k}{k!} L^k, \quad (5)$$

where L^k stands for the resulting operator after k compositions of L . We can also write a representation for the various operator splitting schemes. For example, for the case of the Lie splitting in (3) and by using the expansion in 5,

$$\begin{aligned} e^{\Delta t L_1} e^{\Delta t L_2} &= (I + \Delta t L_1 + o(\Delta t^2)) \cdot (I + \Delta t L_2 + o(\Delta t^2)) \\ &= I + \Delta t L + \frac{\Delta t^2}{2} (L_1^2 + L_2^2 + 2L_1 L_2) + o(\Delta t^2) \end{aligned} \quad (6)$$

Then, the representations in (5) and (6) allow us to study the local error between $P_{\Delta t}$ and $Q_{\Delta t}$:

$$P_{\Delta t}(\sigma, \sigma') - Q_{\Delta t}(\sigma, \sigma) = \frac{\Delta t^2}{2} [L_1, L_2] \delta_{\sigma'}(\sigma) + o(\Delta t^2), \quad (7)$$

where $[L_1, L_2]$ is the *Lie bracket* of L_1, L_2 , and is equal to $L_1 L_2 - L_2 L_1$. Similarly, the order of the local error p is equal to 2. Note that L_1, L_2 can be expressed in terms of the transition rates, which implies that $[L_1, L_2]$ is computable for any pair of states (σ, σ') . A generalization of this idea is in Lemma 1.

Lemma 1 (Commutator and Order of Local Error). *Let σ, σ' be states, $P_{\Delta t}$ as in Equation (1) and $Q_{\Delta t}$: approximation of $P_{\Delta t}$ via a splitting scheme. Then, there is a function $C : S \times S \rightarrow \mathbb{R}$ and an integer $p, p > 1$, such that*

$$P_{\Delta t}(\sigma, \sigma') - Q_{\Delta t}(\sigma, \sigma') = C(\sigma, \sigma') \Delta t^p + o(\Delta t^p). \quad (8)$$

C will be called the **commutator** and p is the **order of the local error**.

Proof. Equation (8) can be derived from the power series representations of $P_{\Delta t}, Q_{\Delta t}$, when L is a bounded operator. \square

In the context of Parallel KMC, the commutator term $C = C(\sigma, \sigma')$ captures the error due to mismatches on the boundary regions between the different sublattices [11].

The operating assumption in this work is that all operators are bounded. This allows us to represent the transition probabilities with power series and,

subsequently, to calculate the form of the commutators and of other quantities of interest. However, the present work could also be extended to the case of unbounded operators [23, 24], where alternative representations for the semigroups could be used for the error analysis. We are not handling such cases here, as the Markov generators of stochastic particle systems are bounded operators [11].

3. Entropy Production Rate: an information criterion for reversibility

Let us consider a discrete stochastic process X_n , $n \in \mathbb{N}$. Then, X_n is time-reversible if, for any $m \in \mathbb{N}$

$$p(\sigma_0, \dots, \sigma_m) = p(\sigma_m, \dots, \sigma_0), \quad (9)$$

where $p(\sigma_0, \dots, \sigma_m) = p(X_0 = \sigma_0, \dots, X_m = \sigma_0)$, σ_i being states of the process. For stationary Markov processes, the detailed balance condition (DB) is equivalent to time-reversibility [25, Theorem 1.2]. If X_n has transition probability P and stationary distribution μ , then DB requires that for all states $\sigma, \sigma' \in S$,

$$\mu(\sigma)P(\sigma, \sigma') = \mu(\sigma')P(\sigma', \sigma). \quad (10)$$

Although the DB condition (10) is a useful analytical tool for the construction of Markov Chains with a specific stationary distribution, we cannot apply it to quantify the loss of reversibility for the systems we are interested in. In our context, P corresponds to the transition probability, $Q_{\Delta t}$, of the scheme, which we do not know explicitly, and $\mu = \mu_Q$ would be the stationary distribution associated with the scheme, which we can only access through sampling. In addition, since such parallel schemes are not exact [5], we do not expect them to exactly satisfy condition (10). For example, approximation may completely break down reversibility, as shown in the case of numerical schemes for SDEs [14]. Instead, we wish to quantify that loss of reversibility and connect it to the parameters of the scheme (lattice decomposition, computation schedule, time step Δt , etc.). Therefore, we need to look for alternative ways to assess the loss of reversibility of the scheme.

Returning to the definition of time-reversibility in (9) with respect to paths, we introduce an object from information theory, the entropy production (EP) associated with P :

$$\text{EP}(P) = \sum_{\sigma_0, \dots, \sigma_m} p(\sigma_0, \dots, \sigma_m) \log \left(\frac{p(\sigma_0, \dots, \sigma_m)}{p(\sigma_m, \dots, \sigma_0)} \right), \quad (11)$$

with the sum in Equation (11) being over S^m , S is the state space.

The EP is an example of a more general measure of similarity between distributions known as the relative entropy (RE), or Kullback-Leibler divergence [26].

Given two probability distributions, p_1 , p_2 , where p_1 is absolutely continuous with respect to p_2 , then the RE of p_1 with respect to p_2 is defined as

$$R(p_1\|p_2) := \int \log \frac{dp_1}{dp_2} dp_1. \quad (12)$$

The definition in (12) enjoys the properties of a divergence: 1. $R(p_1\|p_2) \geq 0$ (Gibbs' inequality), 2. $R(p_1\|p_2) = 0$ if and only if $p_1 = p_2$, p_1 - a.e. However, RE is not a metric in the strict sense, as it does not satisfy the triangle inequality and is not symmetric in its arguments.

From the second property of a divergence, we can readily see that

$$\text{EP}(P) = 0 \Leftrightarrow p(\sigma_0, \dots, \sigma_m) = p(\sigma_m, \dots, \sigma_0). \quad (13)$$

Therefore, if Equation (13) holds for all m , then that implies time-reversibility. It is because of this property of the EP that we will use it as a means to assess and quantify how much a scheme $Q_{\Delta t}$ destroys reversibility. This idea was originally motivated by tools in non-equilibrium statistical mechanics to understand long-time dynamics and fluctuations in associated non-equilibrium steady states [15, 16, 17, 18, 19].

However, calculating the EP, even for moderate m , may seem computationally intensive. But from the definition in (11) we can derive an entropy rate that is independent of the path length, m . By the Markov property, we can write the forward and backward path distributions as

$$\begin{aligned} p(\sigma_0, \dots, \sigma_m) &= \mu(\sigma_0)P(\sigma_0, \sigma_1) \cdots P(\sigma_{m-1}, \sigma_m), \\ p(\sigma_m, \dots, \sigma_0) &= \mu(\sigma_m)P(\sigma_m, \sigma_{m-1}) \cdots P(\sigma_1, \sigma_0), \end{aligned} \quad (14)$$

where μ is the corresponding stationary distribution. Then, using (14) in Equation (11) and carrying out the calculations leads to

$$\text{EP}(P) = m \cdot \sum_{\sigma_0, \sigma_1} \mu(\sigma_0)P(\sigma_0, \sigma_1) \log \left(\frac{P(\sigma_0, \sigma_1)}{P(\sigma_1, \sigma_0)} \right) = m \cdot \text{EPR}(P). \quad (15)$$

The EPR is the entropy production rate and is defined for discrete time Markov processes as

$$\text{EPR}(P) := \sum_{\sigma, \sigma'} \mu(\sigma)P(\sigma, \sigma') \log \left(\frac{P(\sigma, \sigma')}{P(\sigma', \sigma)} \right). \quad (16)$$

A general definition, applicable to continuous-time Markov processes, can also be given, see [14] for an application in quantifying the loss of reversibility for numerical schemes for SDEs.

The EPR is the quantity of interest in this work and we shall apply it to quantifying the loss of reversibility of the schemes studied. First of all, it can be naturally estimated as an observable during a simulation. Indeed, if we

knew the form of $P(\cdot, \cdot)$ explicitly, we could estimate the EPR in (16) by the Gallavotti-Cohen functional (as done in [14]):

$$\text{EPR}(P) = \lim_{N \rightarrow \infty} \frac{1}{N} \sum_{i=0}^N \log \left(\frac{P(\sigma_i, \sigma_{i+1})}{P(\sigma_{i+1}, \sigma_i)} \right). \quad (17)$$

The quantity on the right hand side of Equation (17) is, under suitable ergodic assumptions, an unbiased statistical estimator of the EPR. The corresponding EPR we would like to compute for a given scheme $Q_{\Delta t}$ with stationary distribution μ_Q is

$$\text{EPR}(Q_{\Delta t}) := \frac{1}{\Delta t} \sum_{\sigma, \sigma'} \mu_Q(\sigma) Q_{\Delta t}(\sigma, \sigma') \log \left(\frac{Q_{\Delta t}(\sigma, \sigma')}{Q_{\Delta t}(\sigma', \sigma)} \right). \quad (18)$$

Remark 1. In (18) we normalize with the time step Δt since EPR is a quantity defined as entropy production per unit time, e.g. (15). In this sense, the normalization is also practically important, since we wish to consider comparisons of EPRs for different time-steps Δt . Finally, the same normalization was considered for the RER in [12, Remark 3.2] and Equation (22).

The EP can also be seen as an information criterion for operator splitting schemes. Consider two schemes, $Q_{\Delta t}^1, Q_{\Delta t}^2$ that approximate the same exact $P_{\Delta t}$. Then we can use EP to quantify which of the two retains more reversibility per time step. That is, we are also interested in making statements of the form

$$EP(Q_{\Delta t}^1) \leq EP(Q_{\Delta t}^2). \quad (19)$$

In other words, $EP(Q_{\Delta t}^1) - EP(Q_{\Delta t}^2)$ is an information criterion that takes into account loss of reversibility, similarly to how AIC and BIC are used to assess the quality of models in statistics [27, 28]. However, it remains a difficult quantity to compute. Fortunately, through the EPR and Equation (15), we have another way to distinguish possible schemes based on their performance in controlling the loss of reversibility. In analogy with Inequality (19), we are interested in the difference

$$\text{EPR}(Q_{\Delta t}^1) - \text{EPR}(Q_{\Delta t}^2) \quad (20)$$

for two schemes, $Q_{\Delta t}^1, Q_{\Delta t}^2$. See Figure 3 for a comparison of EPRs.

Even though we have an abstract representation of $Q_{\Delta t}$ (see Equations (3) and (4)), we cannot calculate $Q_{\Delta t}$ directly. What we do know explicitly are the transition rates of the process. We can leverage this information to construct a series expansion of $Q_{\Delta t}$ around Δt where each term depends on the transition rates. Through this, we can build statistical estimators of the highest order terms in an expansion of the EPR. Details about the coefficients and their statistical estimation are in Sections 4, 5. In Figure 3 we demonstrate a comparison of two different parallel KMC schemes, based on these computable *a posteriori* expansions of EPR.

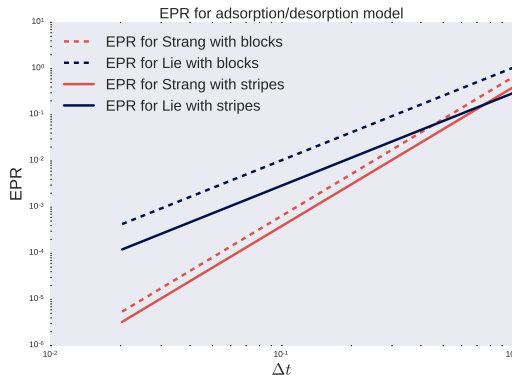


Figure 3: Comparison of two parallel schemes implemented in SPPARKS under two different lattice decompositions with respect to an approximation of the entropy production per unit time (normalized by its scaling with respect to the system size). The Strang scheme retains more reversibility per time step and is more “stable” (with respect to the entropy production rate) under changes in the decomposition. See Section 4 for the discussion about the estimators. Also, note that the estimate is normalized by Δt as per Remark 1.

4. Loss of reversibility in Parallel KMC

In this section, we will demonstrate how to use the EPR to quantify and control the loss of reversibility for parallel Kinetic Monte Carlo (P-KMC). We will also mention details about the implementation of the various observables that are needed in order to estimate EPR.

As mentioned before, for stochastic particle dynamics, we cannot directly apply the definition in Equation (18), as we do not have the transition probabilities $Q_{\Delta t}$ explicitly. Instead, we will use asymptotic results to approximate the EPR for a small splitting time step, Δt (see Section 5 for derivations).

We first write the EPR as per Theorem 1, Section 5, but taking also into consideration Remark 1. That is,

$$\text{EPR}(Q_{\Delta t}) = H(Q_{\Delta t}|P_{\Delta t}) + I(Q_{\Delta t}|P_{\Delta t}), \quad (21)$$

where H represents the relative entropy rate (RER)

$$H(Q_{\Delta t}|P_{\Delta t}) := \frac{1}{\Delta t} \sum_{\sigma, \sigma'} \mu_Q(\sigma) Q_{\Delta t}(\sigma, \sigma') \log \left(\frac{Q_{\Delta t}(\sigma, \sigma')}{P_{\Delta t}(\sigma, \sigma')} \right) \quad (22)$$

and I is a “discrepancy” term (see Section 5) defined as

$$I(Q_{\Delta t}|P_{\Delta t}) := \frac{1}{\Delta t} \sum_{\sigma, \sigma'} \mu_Q(\sigma) Q_{\Delta t}(\sigma, \sigma') \log \left(\frac{P_{\Delta t}(\sigma', \sigma)}{Q_{\Delta t}(\sigma', \sigma)} \right). \quad (23)$$

Before we move on to how results on the RER and I combine to give an asymptotic picture of the EPR, we shall first discuss what each of those captures.

The RER, or relative entropy per unit time, has been used in our previous work [12] as a means to quantify the long-time error of operator splitting schemes in the context of parallel KMC. Because of this, the RER can be used as an information criterion to compare such schemes, as it takes into account details of the scheme such as the splitting time step, the domain decomposition of the lattice, and the computational schedule used. The RER has the properties of a divergence, i.e. non-negativity for any $Q_{\Delta t}, P_{\Delta t}$, and equality with zero if and only if $Q_{\Delta t} = P_{\Delta t}$. The discrepancy term in Equation (23) is what enforces the property of the EPR to be zero when $Q_{\Delta t}$ is time-reversible. As we shall see in Section 5, I is not a divergence.

Now, by the individual results for the asymptotic behavior of RER and I for small Δt , we have

$$H(Q_{\Delta t}|P_{\Delta t}) = A \cdot \Delta t^{p-1} + o(\Delta t^{p-1}), \quad (24)$$

$$I(Q_{\Delta t}|P_{\Delta t}) = D \cdot \Delta t^{p-1} + o(\Delta t^{p-1}). \quad (25)$$

For the RER, the expansion is derived as part of [12], whereas for I the relevant result is Equation (40) in Section 5. Therefore, from Equations (21), (24), and (25), we get

$$\text{EPR}(Q_{\Delta t}) = (A + D)\Delta t^{p-1} + o(\Delta t^{p-1}). \quad (26)$$

We remind here that p stands for the order of the local error (see Lemma 1).

Coefficients A and D are expected values of specific observables with respect to μ_Q (see Appendix C for the explicit formulas in the case of an adsorption/desorption process and Appendix D for the case of a diffusion process). Therefore, under some ergodicity assumptions, they can be estimated via simulation of the system by using the parallel algorithm.

In previous work [12], we expressed A explicitly in terms of the commutator C and the transition rates of the original process. For example, given a lattice Λ , for the Lie splitting and the adsorption/desorption example, the highest order coefficient for the RER is:

$$A = A_{\text{Lie}} = \mathbb{E}_{\mu_{\text{Lie}}} \left[\sum_{x,y \in \Lambda} C_{\text{Lie}}(\sigma, \sigma^{x,y}) F_{\text{Lie}}(\sigma, \sigma^{x,y}) \right] \quad (27)$$

$$= \sum_{\sigma} \mu_{\text{Lie}}(\sigma) \sum_{x,y \in \Lambda} C_{\text{Lie}}(\sigma, \sigma^{x,y}) F_{\text{Lie}}(\sigma, \sigma^{x,y}), \quad (28)$$

where μ_{Lie} is the corresponding stationary distribution of the Lie scheme, $C_{\text{Lie}} = [L_1, L_2]$ and F_{Lie} depends only on the transition rates. Note that A_{Lie} in Equation (27) seemingly depends on all lattice positions x, y . This is also the case for D_{Lie} and the corresponding coefficients for the Strang splitting (see Appendix B). However, an important property of the commutator in Lemma 1 can be used to simplify the situation, explained in Remark 2.

Remark 2. *A key result in [11] was that the commutator is non-zero only for lattice sites on the boundary regions (see Figure 1). This has two major implications:*

1. The sums over the lattice Λ in the highest order coefficients, A and D (see Equation (24) and (25)), are really sums over the boundary regions.
2. We can compute exactly the scaling of the highest order coefficients with the system size.

By Remark 2, we can estimate the EPR in a manner that does not depend on the system size by normalizing by the appropriate scaling. For instance, for the adsorption/desorption system on an $N \times N$ lattice, since the boundary scales as $O(N)$, A_{Lie} in (27) scales like $O(N)$ too [11]. Case in point, for the adsorption/desorption example and the Lie splitting, the per-particle highest order coefficient of the RER (appearing in Equation (24) as “ A ”) would be A_{Lie}/N . We do this for all estimates in this work, i.e. they are per-lattice size estimates.

4.1. Impact of lattice decomposition on reversibility retention

One of the choices a practitioner has to make when using parallel lattice KMC is the decomposition of the lattice, for example checkerboard versus stripes (see Figures 1, 2). Selecting the right decomposition can affect the load-balancing of the algorithm as well as the feasibility of the run. For instance, it may be that the size of the lattice is large enough to prohibit even loading the whole system into the memory of a processor. Then, splitting the lattice into blocks, as in Figure 1, can often bypass this issue, whereas splitting into stripes may not be advantageous.

However, the choice of decomposition has an effect on the error the splitting method generates per time step, both for bounded time intervals [11] and for long simulations [12]. This error is controlled by the commutator associated with the scheme, and the analysis in [11] shows that a decomposition into stripes results to reduced error due to the smaller size of the boundary region. By approximating the EPR, we can quantify the long-time effect such a change has to the reversibility each scheme retains per time step. To discuss those issues, we simulated an adsorption/desorption process and used the samples to estimate the EPR. For details about the setup of the example, see Appendix C.

In Figure 3, we can see how *sensitive* is each scheme to different decompositions of the lattice. Note that in both cases, the schemes have a smaller EPR estimate when using a stripe versus a block decomposition. In fact, the Strang scheme has consistently better performance in controlling the loss of reversibility with respect to Δt .

Decomposing the estimate of the EPR (used in Figure 3) for the Lie splitting to the RER and discrepancy components gives Figure 4. Figure 5 shows the same comparison for Strang. We note that the part most affected by the change in decomposition is the discrepancy (Equation (23)). As expected by Figure 3, we have that the Strang splitting is more stable with respect to the switch of decomposition.

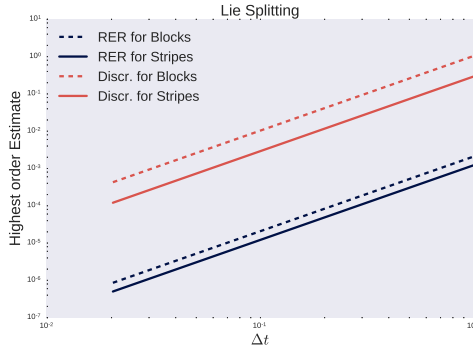


Figure 4: Approximations to the RER and the discrepancy for the same system as with Figure 3 for the Lie splitting (normalized with respect to the system size). Lie seems more sensitive to changes in the decomposition of the lattice. Both the RER (Equation (22)) and the discrepancy (Equation (23)) are normalized by Δt , see Remark 1.

5. Derivations and General Theory

In this section, we present the general theory concerning the asymptotic behavior of the entropy production rate (EPR) of a scheme $Q_{\Delta t}$. The arguments presented here, although mirroring some of the ideas from our previous work [12], also take into account the additional discrepancy term, $I(Q_{\Delta t}|P_{\Delta t})$. Although we handle only the case that L is split into $L_1 + L_2$, the arguments can also generalize to splittings with more components, e.g. $L_1 + L_2 + L_3$. In fact, the arguments can readily generalize to schemes that are not splittings, as long as there is an expression for the error like the one in Lemma 1. Nevertheless, we will continue to consider splitting methods in this section.

Remark 3. *An implicit assumption in the parallel schemes used in Section 4 was that the splitting of the generator L into $L_1 + L_2$ was such that if $q(\sigma, \sigma') = 0$ for some pair of states (σ, σ') , then $q_1(\sigma, \sigma') = q_2(\sigma, \sigma') = 0$. This is imposed by the domain decomposition of the lattice and we also assume this throughout for any splitting of L , although the methodology can be extended to other splittings too.*

5.1. Decomposition of the Entropy Production Rate

To better understand the Entropy Production Rate, we shall first decompose it into two pieces, the relative entropy rate, Equation (22), and a “discrepancy” term (Equation (23)) that we will denote with I .

Theorem 1. *Let $\Delta t > 0$ and $P_{\Delta t}$ be a transition probability, with stationary distribution μ , that satisfies detailed balance. Then, if $Q_{\Delta t}$ is an approximation coming from a numerical scheme, we have that*

$$\text{EPR}(Q_{\Delta t}) = H(Q_{\Delta t}|P_{\Delta t}) + I(Q_{\Delta t}|P_{\Delta t}). \quad (21)$$

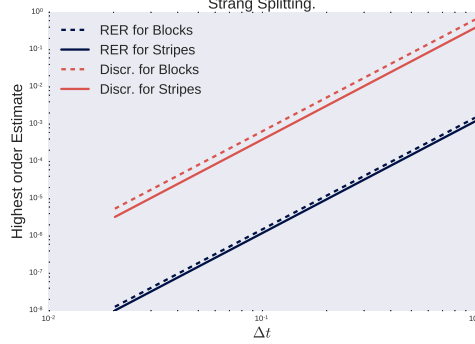


Figure 5: Approximations to the RER and the discrepancy for the same system as with Figure 3 for the Strang splitting (normalized with respect to the system size). Both the discrepancy and the RER are less affected by switching from blocks to stripes when using the Strang splitting. Both the RER (Equation (22)) and the discrepancy (Equation (23)) are normalized by Δt , see Remark 1.

Proof. Earlier we defined the *entropy production rate* corresponding to $Q_{\Delta t}$ as

$$\text{EPR}(Q_{\Delta t}) = \frac{1}{\Delta t} \sum_{\sigma, \sigma'} \mu_Q(\sigma) Q_{\Delta t}(\sigma, \sigma') \log \left(\frac{Q_{\Delta t}(\sigma, \sigma')}{Q_{\Delta t}(\sigma', \sigma)} \right), \quad (16)$$

We will first introduce the reversible $P_{\Delta t}$ in Equation (16) as

$$\Delta t \cdot \text{EPR}(Q_{\Delta t}) = \sum_{\sigma, \sigma', \sigma' \neq \sigma} \mu_Q(\sigma) Q_{\Delta t}(\sigma, \sigma') \log \left(\frac{Q_{\Delta t}(\sigma, \sigma') P_{\Delta t}(\sigma, \sigma') P_{\Delta t}(\sigma', \sigma)}{P_{\Delta t}(\sigma, \sigma') P_{\Delta t}(\sigma', \sigma) Q_{\Delta t}(\sigma', \sigma)} \right).$$

This allows us to split the logarithm into three pieces.

$$\begin{aligned} \Delta t \cdot \text{EPR}(Q_{\Delta t}) &= \sum_{\sigma, \sigma'} \mu_Q(\sigma) Q_{\Delta t}(\sigma, \sigma') \log \left(\frac{Q_{\Delta t}(\sigma, \sigma')}{P_{\Delta t}(\sigma, \sigma')} \right) \\ &\quad + \sum_{\sigma, \sigma'} \mu_Q(\sigma) Q_{\Delta t}(\sigma, \sigma') \log \left(\frac{P_{\Delta t}(\sigma, \sigma')}{P_{\Delta t}(\sigma', \sigma)} \right) \\ &\quad + \sum_{\sigma, \sigma'} \mu_Q(\sigma) Q_{\Delta t}(\sigma, \sigma') \log \left(\frac{P_{\Delta t}(\sigma', \sigma)}{Q_{\Delta t}(\sigma', \sigma)} \right). \end{aligned} \quad (29)$$

We shall now show that the middle sum is equal to zero. By our assumptions, we know that the pair $(P_{\Delta t}, \mu)$ satisfies detailed balance, i.e. $\mu(\sigma')/ \mu(\sigma) = P_{\Delta t}(\sigma, \sigma')/ P_{\Delta t}(\sigma', \sigma)$. Therefore,

$$\sum_{\sigma, \sigma'} \mu_Q(\sigma) Q_{\Delta t}(\sigma, \sigma') \log \left(\frac{P_{\Delta t}(\sigma, \sigma')}{P_{\Delta t}(\sigma', \sigma)} \right) = \sum_{\sigma, \sigma'} \mu_Q(\sigma) Q_{\Delta t}(\sigma, \sigma') [\log(\mu(\sigma')) - \log(\mu(\sigma))]. \quad (30)$$

Looking at each sum in Equation (30) separately and using that $\mu_Q(\sigma') = \sum_{\sigma} \mu_Q(\sigma) Q_{\Delta t}(\sigma, \sigma')$, we have

$$\begin{aligned} \sum_{\sigma} \sum_{\sigma'} \mu_Q(\sigma) Q_{\Delta t}(\sigma, \sigma') \log(\mu(\sigma')) &= \sum_{\sigma'} \mu_Q(\sigma') \log(\mu(\sigma')), \\ \sum_{\sigma} \sum_{\sigma'} \mu_Q(\sigma) Q_{\Delta t}(\sigma, \sigma') \log(\mu(\sigma)) &= \sum_{\sigma} \mu_Q(\sigma) \log(\mu(\sigma)). \end{aligned}$$

Thus, Equation (30) is equal to zero and we have,

$$\begin{aligned} \Delta t \cdot \text{EPR}(Q_{\Delta t}) &= \sum_{\sigma, \sigma'} \mu_Q(\sigma) Q_{\Delta t}(\sigma, \sigma') \log \left(\frac{Q_{\Delta t}(\sigma, \sigma')}{P_{\Delta t}(\sigma, \sigma')} \right) \\ &\quad + \sum_{\sigma, \sigma'} \mu_Q(\sigma) Q_{\Delta t}(\sigma, \sigma') \log \left(\frac{P_{\Delta t}(\sigma', \sigma)}{Q_{\Delta t}(\sigma', \sigma)} \right). \end{aligned}$$

or

$$\text{EPR}(Q_{\Delta t}) = (H(Q_{\Delta t}|P_{\Delta t}) + I(Q_{\Delta t}|P_{\Delta t}))/\Delta t.$$

□

Note that, even though the EPR and the RER are always non-negative, the discrepancy, I , is not. If $Q_{\Delta t}$ is reversible, then $\text{EPR}(Q_{\Delta t}) = 0 \Rightarrow H(Q_{\Delta t}|P_{\Delta t}) = -I(Q_{\Delta t}|P_{\Delta t})$. If, in addition, $Q_{\Delta t} \neq P_{\Delta t}$, then the RER is strictly positive, which implies that I would be negative.

5.2. Asymptotic Behavior of Entropy Production Rate

In Theorem 1 we saw that we can express the entropy production rate (EPR) of a scheme as a sum of two different components, the relative entropy rate (RER) and the discrepancy (Equation (23)). The objective of this section is the study of each component separately via asymptotic expansions with respect to Δt . Then, at the end of the section we have an asymptotic result for the EPR.

In the derivations that follow, we will often refer to the distances between different states of the state space, as measured by

$$d(\sigma, \sigma') := \begin{cases} \min\{|\vec{z}| : \vec{z} \in \text{Path}(\sigma \rightarrow \sigma')\}, & \text{Path}(\sigma \rightarrow \sigma') \neq \emptyset, \\ \infty, & \text{Path}(\sigma \rightarrow \sigma') = \emptyset, \end{cases} \quad (31)$$

with $|\vec{z}|$ being an integer that denotes the number of jumps in the path \vec{z} and $\text{Path}(\sigma \rightarrow \sigma')$ being the set of all possible paths between the two states which have a positive probability. The mapping d is also known as the geodesic distance and is always calculated with respect to the transition rates q of the exact process. Also, in the case of a reversible system, d is a metric of the state space, as it is symmetric and satisfies the triangle inequality. Once we have d , we can also define the *diameter* of the system as $\text{diam}(S) = \max_{(\sigma, \sigma') \in S \times S} \{d(\sigma, \sigma')\}$.

We introduced the use of the geodesic distance (31) in [12]. For schemes that satisfy the requirement in Remark 3, the addition of this graph-theoretic perspective can both simplify and generalize the computations. For completeness, we include the result concerning the long-time behavior of the scheme with respect to the RER [12, Theorem 5.6], the only difference being that in Lemma 2, we state the result for $H(Q_{\Delta t}|P_{\Delta t})$ instead of the time-step normalized version (see Remark 1).

Lemma 2. *Let $P_{\Delta t}(\sigma, \sigma') = e^{L\Delta t}\delta_{\sigma'}(\sigma)$ and $Q_{\Delta t}(\sigma, \sigma')$ be an approximation of $P_{\Delta t}$ based on a splitting scheme and μ_Q the stationary measure corresponding to $Q_{\Delta t}$. Then, if the scheme is of order p , we define the bounded diameter of the state space as \hat{k} ,*

$$\hat{k} = \min\{\text{diam}(S), p\} = \min\{\max_{\sigma, \sigma'}\{d(\sigma, \sigma')\}, p\}.$$

Then, if $C(\sigma, \sigma') \neq 0$ for at least one pair $\sigma, \sigma' \in S$ such that $d(\sigma, \sigma') = \hat{k}$, we have that

$$H(Q_{\Delta t}|P_{\Delta t}) = O(\Delta t^{2p-(\hat{k}+1)}).$$

Note that in Apart from giving us scaling for the RER and a connection with the commutator, C , and the order of the local error p (see Lemma 1), Lemma 2 also provided an approximation of the RER for small Δt , as the highest order term can be written explicitly with respect to the original transition rates of the system. As we will see next, a similar line of thinking can provide results for the discrepancy term. Lemma 3 provides a result for the special case that $\hat{k} = p$, which is the usual case for stochastic particle systems.

Lemma 3. *Under the assumptions of Lemma 2 and for $\hat{k} = p$,*

$$I(Q_{\Delta t}|P_{\Delta t}) = O(\Delta t^{p-1}).$$

Proof. Earlier we defined the discrepancy:

$$\Delta t \cdot I(Q_{\Delta t}|P_{\Delta t}) = \sum_{\sigma, \sigma'} \mu_Q(\sigma) Q_{\Delta t}(\sigma, \sigma') \log \left(\frac{P_{\Delta t}(\sigma', \sigma)}{Q_{\Delta t}(\sigma', \sigma)} \right). \quad (32)$$

The goal is to separate Equation (32) into pieces and then expose the dependence to Δt . Using the atanh representation of the logarithm [12] and its expansion we get that

$$\Delta t \cdot I(Q_{\Delta t}|P_{\Delta t}) = \sum_{\sigma, \sigma'} \mu_Q(\sigma) Q_{\Delta t}(\sigma, \sigma') \cdot 2 \sum_{k=0}^{\infty} \frac{1}{2k+1} \left(\frac{P_{\Delta t}(\sigma', \sigma) - Q_{\Delta t}(\sigma', \sigma)}{Q_{\Delta t}(\sigma', \sigma) + P_{\Delta t}(\sigma', \sigma)} \right)^{2k+1}. \quad (33)$$

A result from the proof of Lemma 2 [12, Lemma 3.5] that we will use concerns the asymptotic behavior of ratios. That is,

$$\frac{P_{\Delta t}(\sigma', \sigma) - Q_{\Delta t}(\sigma', \sigma)}{P_{\Delta t}(\sigma', \sigma) + Q_{\Delta t}(\sigma', \sigma)} = \frac{C(\sigma', \sigma)}{2Q_{\Delta t}(\sigma', \sigma) + C(\sigma', \sigma)\Delta t^p} \Delta t^p + o(\Delta t^p). \quad (34)$$

We assume that all σ, σ' satisfy $d(\sigma, \sigma') = p$, i.e. they are p jumps apart. Next, we define

$$M(\sigma, \sigma') = \frac{C(\sigma, \sigma')}{C(\sigma, \sigma') + 2L_Q^p(\sigma, \sigma')/p!}, \quad (35)$$

where L_Q^p represents all the terms in the expansion of $Q_{\Delta t}$ that are of order p (see Equation (B.2) in appendix). Then for $k > 0$, we have that

$$\begin{aligned} & \sum_{\sigma, \sigma'} \mu_Q(\sigma) Q_{\Delta t}(\sigma, \sigma') \cdot 2 \sum_{k=1}^{\infty} \frac{1}{2k+1} \left(\frac{P_{\Delta t}(\sigma', \sigma) - Q_{\Delta t}(\sigma', \sigma)}{P_{\Delta t}(\sigma', \sigma) + Q_{\Delta t}(\sigma', \sigma)} \right)^{2k+1} \\ &= \sum_{\sigma, \sigma'} \mu_Q(\sigma) L_Q^p(\sigma, \sigma') \frac{2\Delta t^p}{p!} (\operatorname{atanh}(M(\sigma', \sigma)) - M(\sigma', \sigma)) + o(\Delta t^p). \end{aligned} \quad (36)$$

Before we continue with the analysis of Equation (36), we look at the term from Equation (33) corresponding to $k = 0$. Using Equation (34), we get

$$2 \sum_{\sigma, \sigma'} \mu_Q(\sigma) Q_{\Delta t}(\sigma, \sigma') \cdot \frac{C(\sigma', \sigma)}{2Q_{\Delta t}(\sigma', \sigma) + C(\sigma', \sigma)\Delta t^p} \Delta t^p + o(\Delta t^p). \quad (37)$$

We notice that to get terms of order Δt^p from the sum (37), we need the order of $Q_{\Delta t}(\sigma, \sigma')$ to be the same as that of $Q_{\Delta t}(\sigma', \sigma)$. We remind here that the order of the local error is equal to p and that L^i is the resulting operator after i compositions of the generator of the original chain L . Therefore, if $i < p$, the ratio

$$\frac{Q_{\Delta t}(\sigma, \sigma')}{Q_{\Delta t}(\sigma', \sigma)} = \frac{L^i(\sigma, \sigma')}{L^i(\sigma', \sigma)} + o(\Delta t) \quad (38)$$

is well defined as long as $L^i(\sigma, \sigma') \neq 0$. From Lemma 4, we have that if $d(\sigma, \sigma') = i \Rightarrow L^i(\sigma, \sigma') \neq 0$. Therefore, Equation (38) is well-defined for all σ, σ' such that $d(\sigma, \sigma') = i, i < p$. This finalizes the analysis of the first term of the asymptotic series for I , with

$$\begin{aligned} & 2 \sum_{\sigma, \sigma'} \mu_Q(\sigma) Q_{\Delta t}(\sigma, \sigma') \cdot \frac{C(\sigma', \sigma)}{2Q_{\Delta t}(\sigma', \sigma) + C(\sigma', \sigma)\Delta t^p} \Delta t^p + o(\Delta t^p) \\ &= \sum_{\sigma} \mu_Q(\sigma) \sum_{i=0}^{p-1} \sum_{\sigma' \in S_i(\sigma)} \frac{L^i(\sigma, \sigma')}{L^i(\sigma', \sigma)} C(\sigma', \sigma) \\ & \quad + \sum_{\sigma' \in S_p(\sigma)} L_Q^p(\sigma, \sigma') \frac{2}{p!} M(\sigma', \sigma) \Delta t^p + o(\Delta t^p). \end{aligned} \quad (39)$$

Above we use the notation $S_i(\sigma) = \{\sigma' : d(\sigma, \sigma') = i\}$, where d is the geodesic distance from Equation (31). Now, if we add Equations (36) and (39), the terms

that involve $M(\sigma', \sigma)$ cancel. Therefore, we get the following asymptotic result for I .

$$\begin{aligned}
I(Q_{\Delta t}|P_{\Delta t}) &= \sum_{\sigma} \mu_Q(\sigma) \sum_{i=0}^{p-1} \sum_{\sigma' \in S_i(\sigma)} \frac{L^i(\sigma, \sigma')}{L^i(\sigma', \sigma)} C(\sigma', \sigma) \Delta t^{p-1} \\
&+ \sum_{\sigma, \sigma' \in S_p(\sigma)} \mu_Q(\sigma) L_Q^p(\sigma, \sigma') \frac{2}{p!} \operatorname{atanh}(M(\sigma', \sigma)) \Delta t^{p-1} \\
&+ o(\Delta t^{p-1}).
\end{aligned} \tag{40}$$

□

Equation (40) is the basis for our estimation of I for small Δt , which is used in Section 4. The following lemma is used in the proof.

Lemma 4. *Let σ, σ' be states such that $d(\sigma, \sigma') = k \in \mathbb{N}$. Then, $L^k(\sigma, \sigma') > 0$.*

Proof. You can find the statement and proof in Lemma 7 at Appendix A. □

An immediate implication of Theorem 1 and Lemmas 2 and 3 is the next result, which provides the scaling of the EPR with respect to Δt .

Theorem 2. *Let $\Delta t \in (0, 1)$. Let $P_{\Delta t}(\sigma, \sigma') = e^{L\Delta t} \delta_{\sigma'}(\sigma)$ and $Q_{\Delta t}(\sigma, \sigma')$ be an approximation of $P_{\Delta t}$ based on a splitting scheme and μ_Q the stationary measure corresponding to $Q_{\Delta t}$. In addition, let $P_{\Delta t}$ satisfy detailed balance and $\operatorname{diam}(S) \geq p$. Then,*

$$\operatorname{EPR}(Q_{\Delta t}) = O(\Delta t^{p-1}).$$

6. Conclusions

We introduced the entropy production rate (EPR) as a means to quantify the loss of reversibility for operator splitting schemes applied to Parallel Kinetic Monte Carlo. We showed estimation of the EPR does not require the knowledge of the stationary distribution and depends on the transition probabilities of the scheme. Since the transition probabilities for stochastic particle systems are usually not available, or difficult to explicitly compute, we derived *a posteriori* estimators of the EPR and connected the parameters of the scheme with a quantitative assessment of the loss of reversibility. We demonstrated this fact with an application to lattice KMC with adsorption/desorption dynamics, which we simulated using SPPARKS [9], and a comparison between two splitting schemes, Lie and Strang. We demonstrated that the Strang splitting retains more reversibility per time step compared to Lie and is more stable with respect to changes in the decomposition of the lattice (blocks versus stripes, see Figure 3).

The proposed framework for Parallel KMC, can be applied to more than computational schedule comparison. In essence, the EPR can be used as an information criterion that allows practitioners to judge the fine details of the

scheme itself, like the time step and which lattice decompositions retain more reversibility (see Figure 3). The EPR can also be used as a diagnostic observable to assess the reversibility of the scheme used by simulating a system of smaller size than the one of interest. In this way, issues with the scheme can be discovered early on using a much smaller system for diagnostics, different schemes can be compared, and parameters tuned to minimize the loss of reversibility.

Though we only considered operator splitting schemes in the context of parallel lattice KMC, the idea of using the EPR for the quantification of the loss of reversibility can be used on other schemes too, as long as an expression for their local error exists and is computable. For instance, an extension of this work can be used to quantify the loss of reversibility for schemes used for thermostated Molecular Dynamics simulations [29], for example for Langevin dynamics [30].

Acknowledgments

The work of KG and MAK was partially supported by the Office of Advanced Scientific Computing Research, U.S. Department of Energy, under Contract No. DE-SC0010723. The work of LRB was partially supported by the Office of Advanced Scientific Computing Research, U.S. Department of Energy, under Contract No. DE-SC0010723 and the National Science Foundation under Grant No. DMS 1515172.

References

References

- [1] Alfred B Bortz, Malvin H Kalos, and Joel L Lebowitz. A new algorithm for monte carlo simulation of ising spin systems. *Journal of Computational Physics*, 17(1):10–18, 1975.
- [2] Malvin H. Kalos and Paula A. Whitlock. *Monte Carlo Methods*. Wiley-Interscience, New York, NY, USA, 1986.
- [3] David Landau and Kurt Binder. *A Guide to Monte Carlo Simulations in Statistical Physics*. Cambridge University Press, New York, NY, USA, 2005.
- [4] Boris D Lubachevsky. Efficient parallel simulations of dynamic ising spin systems. *Journal of Computational Physics*, 75(1):103–122, 1988.
- [5] Yunsic Shim and Jacques G. Amar. Semirigorous synchronous sublattice algorithm for parallel kinetic monte carlo simulations of thin film growth. *Phys. Rev. B*, 71:125432, Mar 2005.
- [6] E. Martnez, J. Marian, M.H. Kalos, and J.M. Perlado. Synchronous parallel kinetic monte carlo for continuum diffusion-reaction systems. *Journal of Computational Physics*, 227(8):3804 – 3823, 2008.

- [7] NJ van der Kaap and LJA Koster. Massively parallel kinetic monte carlo simulations of charge carrier transport in organic semiconductors. *Journal of Computational Physics*, 307:321–332, 2016.
- [8] Eishin Endo, Yuta Toga, and Munetaka Sasaki. Parallelized stochastic cutoff method for long-range interacting systems. *Journal of the Physical Society of Japan*, 84(7):074002, 2015.
- [9] Steve Plimpton, Corbett Battaile, Mike Chandross, Liz Holm, Aidan Thompson, Veena Tikare, Greg Wagner, E Webb, X Zhou, C Garcia Cardona, et al. Crossing the mesoscale no-mans land via parallel kinetic monte carlo. *Sandia Report SAND2009-6226*, 2009.
- [10] Giorgos Arampatzis, Markos A. Katsoulakis, Petr Plecháč, Michela Taufer, and Lifan Xu. Hierarchical fractional-step approximations and parallel kinetic monte carlo algorithms. *J. Comput. Phys.*, 231(23):7795–7814, October 2012.
- [11] Giorgos Arampatzis, Markos A. Katsoulakis, and Petr Plecháč. Parallelization, processor communication and error analysis in lattice kinetic monte carlo. *SIAM Journal on Numerical Analysis*, 52(3):1156–1182, 2014.
- [12] K. Gourgoulias, M. A. Katsoulakis, and L. Rey-Bellet. Information metrics for long-time errors in splitting schemes for stochastic dynamics and parallel kMC. *pre-print*. arXiv:1511.08240 [math.NA].
- [13] Jerome P. Nilmeier and Jaime Marian. A rigorous sequential update strategy for parallel kinetic monte carlo simulation. *Computer Physics Communications*, 185(10):2479 – 2486, 2014.
- [14] Markos Katsoulakis, Yannis Pantazis, and Luc Rey-Bellet. Measuring the irreversibility of numerical schemes for reversible stochastic differential equations. *ESAIM: Mathematical Modelling and Numerical Analysis*, 48:1351–1379, 9 2014.
- [15] Christian Maes. The fluctuation theorem as a gibbs property. *Journal of statistical physics*, 95(1-2):367–392, 1999.
- [16] Christian Maes, Frank Redig, and Annelies Van Moffaert. On the definition of entropy production, via examples. *Journal of Mathematical Physics*, 41(3):1528–1554, 2000.
- [17] Joel L. Lebowitz and Herbert Spohn. A gallavotti–cohen-type symmetry in the large deviation functional for stochastic dynamics. *Journal of Statistical Physics*, 95(1):333–365.
- [18] Jorge Kurchan. Fluctuation theorem for stochastic dynamics. *Journal of Physics A: Mathematical and General*, 31(16):3719, 1998.

- [19] Giovanni Gallavotti and EGD Cohen. Dynamical ensembles in stationary states. *Journal of Statistical Physics*, 80(5-6):931–970, 1995.
- [20] Yannis Pantazis and Markos A. Katsoulakis. A relative entropy rate method for path space sensitivity analysis of stationary complex stochastic dynamics. *The Journal of Chemical Physics*, 138(5), 2013.
- [21] Evangelia Kalligiannaki, Markos A. Katsoulakis, and Petr Plecháč. Spatial two-level interacting particle simulations and information theory–based error quantification. *SIAM Journal on Scientific Computing*, 36(2):A634–A667, 2014.
- [22] H. F. Trotter. On the product of semi-groups of operators. *Proceedings of the American Mathematical Society*, 10(4):pp. 545–551, 1959.
- [23] Eskil Hansen and Alexander Ostermann. Exponential splitting for unbounded operators. *Mathematics of computation*, 78(267):1485–1496, 2009.
- [24] Tobias Jahnke and Derya Altntan. Efficient simulation of discrete stochastic reaction systems with a splitting method. *BIT Numerical Mathematics*, 50(4):797–822, 2010.
- [25] Frank P Kelly. *Reversibility and stochastic networks*. Cambridge University Press, 2011.
- [26] Thomas M. Cover and Joy A. Thomas. *Elements of Information Theory*. Wiley-Interscience, New York, NY, USA, 1991.
- [27] Hirotugu Akaike. Information theory and an extension of the maximum likelihood principle. In Emanuel Parzen, Kunio Tanabe, and Genshiro Kitagawa, editors, *Selected Papers of Hirotugu Akaike*, Springer Series in Statistics, pages 199–213. Springer New York, 1998.
- [28] Hirotugu Akaike. A new look at the bayes procedure. In Emanuel Parzen, Kunio Tanabe, and Genshiro Kitagawa, editors, *Selected Papers of Hirotugu Akaike*, Springer Series in Statistics, pages 281–287. Springer New York, 1998.
- [29] Ben Leimkuhler and Charles Matthews. *Molecular Dynamics: with deterministic and stochastic numerical methods*, volume 39. Springer, 2015.
- [30] Benedict Leimkuhler, Charles Matthews, and Gabriel Stoltz. The computation of averages from equilibrium and nonequilibrium langevin molecular dynamics. *IMA Journal of Numerical Analysis*, 2015.

Appendix A. Supporting Results

In this section, we provide the proofs for any supporting results in the main manuscript.

Let X_n be a Markov process with P the Markov transition probability kernel and μ the corresponding stationary distribution. Also,

$$p(\sigma_0, \dots, \sigma_m) = p(X_0 = \sigma_0, \dots, X_m = \sigma_0),$$

σ_i being states of the process from a state space S . We also use the notation $\sigma_{0:m}$ for the sequence of states $\sigma_0, \dots, \sigma_m$.

Appendix A.1. Connection of the Entropy Production with the Entropy Production Rate

In the main text, we sketched a proof for the connection between entropy production (EP) for paths of length m ,

$$\text{EP}(P) = \sum_{\sigma_{0:m}} p(\sigma_{0:m}) \log \left(\frac{p(\sigma_{0:m})}{p(\sigma_{m:0})} \right), \quad (\text{A.1})$$

and entropy production per unit time (or entropy production rate (EPR)),

$$\text{EPR}(P) = \sum_{\sigma, \sigma'} \mu(\sigma) P(\sigma, \sigma') \log \left(\frac{P(\sigma, \sigma')}{P(\sigma', \sigma)} \right). \quad (\text{A.2})$$

More details about this relation are provided in Lemma 5.

Lemma 5. *let $m \in \mathbb{N}$ and let P be a Markov transition probability kernel, with μ being the stationary distribution that corresponds to P . Then,*

$$\text{EP}(P) = m \cdot \sum_{\sigma_0, \sigma_1} \mu(\sigma_0) P(\sigma_0, \sigma_1) \log \left(\frac{P(\sigma_0, \sigma_1)}{P(\sigma_1, \sigma_0)} \right) = m \cdot \text{EPR}(P). \quad (\text{A.3})$$

Proof. By the Markov property, we can express $p(\sigma_0, \dots, \sigma_m)$, $p(\sigma_m, \dots, \sigma_0)$ with respect to P, μ :

$$\begin{aligned} p(\sigma_{0:m}) &= \mu(\sigma_0) P(\sigma_0, \sigma_1) \cdots P(\sigma_{m-1}, \sigma_m), \\ p(\sigma_{m:0}) &= \mu(\sigma_m) P(\sigma_m, \sigma_{m-1}) \cdots P(\sigma_1, \sigma_0). \end{aligned} \quad (\text{A.4})$$

Substituting those in the definition of the EP in Equation (A.1), we get

$$\begin{aligned} & \sum_{\sigma_{0:m}} \mu(\sigma_0) P(\sigma_0, \sigma_1) \cdots P(\sigma_{m-1}, \sigma_m) \log \left(\frac{\mu(\sigma_0) P(\sigma_0, \sigma_1) \cdots P(\sigma_{m-1}, \sigma_m)}{\mu(\sigma_m) P(\sigma_m, \sigma_{m-1}) \cdots P(\sigma_1, \sigma_0)} \right) \\ &= \sum_{\sigma_{0:m}} \mu(\sigma_0) P(\sigma_0, \sigma_1) \cdots P(\sigma_{m-1}, \sigma_m) \log \left(\frac{\mu(\sigma_0)}{\mu(\sigma_m)} \right) \end{aligned} \quad (\text{A.5})$$

$$+ \sum_{\sigma_{0:m}} \mu(\sigma_0) P(\sigma_0, \sigma_1) \cdots P(\sigma_{m-1}, \sigma_m) \sum_{k=1}^m \log \left(\frac{P(\sigma_{k-1}, \sigma_k)}{P(\sigma_k, \sigma_{k-1})} \right). \quad (\text{A.6})$$

First, we shall show that Equation (A.5) is equal to zero. We can write it as

$$\sum_{\sigma_{0:m}} \mu(\sigma_0) \log(\mu(\sigma_0)) P(\sigma_0, \sigma_1) \cdots P(\sigma_{m-1}, \sigma_m) \quad (\text{A.7})$$

$$- \sum_{\sigma_{0:m}} \mu(\sigma_0) P(\sigma_0, \sigma_1) \cdots P(\sigma_{m-1}, \sigma_m) \log(\mu(\sigma_m)). \quad (\text{A.8})$$

Now, for the first sum, we can repeatedly use that

$$\sum_{\sigma'} P(\sigma, \sigma') = 1 \quad (\text{A.9})$$

for all states σ , which results to Equation (A.7) being reduced to

$$\sum_{\sigma_0} \mu(\sigma_0) \log(\mu(\sigma_0)).$$

For the part in (A.8), since μ is the stationary distribution associated with P , we have that for any state σ' ,

$$\mu(\sigma') = \sum_{\sigma} \mu(\sigma) P(\sigma, \sigma'). \quad (\text{A.10})$$

Using the property in (A.10) repeatedly on Equation (A.8), we get that it is equal to (A.7), which gives the equality of (A.5) to zero. Next, we need to account for (A.6), which we write as

$$\sum_{k=1}^m \sum_{\sigma_{0:m}} \mu(\sigma_0) P(\sigma_0, \sigma_1) \cdots P(\sigma_{m-1}, \sigma_m) \log \left(\frac{P(\sigma_{k-1}, \sigma_k)}{P(\sigma_k, \sigma_{k-1})} \right). \quad (\text{A.11})$$

For $k = 1$, and by using property (A.9), we get

$$\sum_{\sigma_{0:1}} \mu(\sigma_0) P(\sigma_0, \sigma_1) \log \left(\frac{P(\sigma_0, \sigma_1)}{P(\sigma_1, \sigma_0)} \right). \quad (\text{A.12})$$

For any other k in Equation (A.11), we can use Equation (A.10) to show that all terms are equal to (A.12). Since we have m of those, this proves the result. \square

Appendix A.2. Supporting results relating connectivity and Markov generators

We remind here that L is a generator of a Markov process X_n , L^k represents the result of k compositions of L . d is the geodesic distance between states, defined with respect to the transition rates of the exact Markov process with transition probabilities $P_{\Delta t}$:

$$d(\sigma, \sigma') := \begin{cases} \min\{|\vec{z}| : \vec{z} \in \text{Path}(\sigma \rightarrow \sigma')\}, & \text{Path}(\sigma \rightarrow \sigma') \neq \emptyset, \\ \infty, & \text{Path}(\sigma \rightarrow \sigma') = \emptyset. \end{cases} \quad (\text{A.13})$$

In (A.13), $|\vec{z}|$ is the length of a path from σ to σ' and $\text{Path}(\sigma \rightarrow \sigma')$ corresponds to the set of all such possible paths.

One of the results we used in the text was that if we have two states σ, σ' with $d(\sigma, \sigma') = k$, then $L^k(\sigma, \sigma') > 0$. To arrive at this, we first show that L^k has a particular form for those (σ, σ') in Lemma 6.

Lemma 6. *Let $\sigma, \sigma' \in S$ and let L be the generator of the Markov process. Then*

$$d(\sigma, \sigma') = k \Rightarrow L^k(\sigma, \sigma') = \sum_{z_{1:n-1}} q(\sigma, z_1) \dots q(z_{k-1}, \sigma').$$

Note the notation $z_{1:n-1} = (z_1, \dots, z_{n-1})$ for a path of states of length $n-1$.

Proof. The result is immediate for $k=0$ or $k=1$. Then, $L^0(\sigma, \sigma) = \delta_\sigma(\sigma) = 1$ and $L(\sigma, \sigma') = q(\sigma, \sigma')$, since there is only one path between σ and σ' .

Let us assume that this fact holds for $k=n$. That is, for states such that $d(\sigma, \sigma') = n$,

$$L^n(\sigma, \sigma') = \sum_{z_{1:n-1}} q(\sigma, z_1) \dots q(z_{n-1}, \sigma'). \quad (\text{A.14})$$

Note that in Equation (A.14), we have a sum over all paths of length n connecting σ to σ' .

We will now show the result for $d(\sigma, \sigma') = n+1$. Since L^{n+1} is L after $n+1$ compositions, we can write

$$L^{n+1}(\sigma, \sigma') = L[L^n[\delta_{\sigma'}]](\sigma). \quad (\text{A.15})$$

Then, by the definition of the generator L ,

$$\begin{aligned} L[L^n[\delta_{\sigma'}]](\sigma) &= \sum_z q(\sigma, z) (L^n[\delta_{\sigma'}](z) - L^n[\delta_{\sigma'}](\sigma)) \\ &= \sum_z q(\sigma, z) L^n[\delta_{\sigma'}](z) \end{aligned} \quad (\text{A.16})$$

In (A.16), we used that $d(\sigma, \sigma') = n+1 \Rightarrow L^n[\delta_{\sigma'}](\sigma) = 0$. This is true by the induction hypothesis we made in Equation (A.14).

Now, if $q(\sigma, z) = 0$, the corresponding terms are also zero, so let $q(\sigma, z) > 0$, or equivalently $d(\sigma, z) = 1$. It is not difficult to see that in this case

$$n \leq d(z, \sigma') \leq n+2.$$

For the upper bound, we can apply the triangle inequality for d . To get the lower, if $d(\sigma, z) = 1$ and $d(z, \sigma')$ is equal to $n - 1$, then by following the path $\sigma \rightarrow z \rightarrow \sigma'$, we get a new path between σ and σ' with n steps. This contradicts that $d(\sigma, \sigma')$ is the minimum number of steps to get from σ to σ' .

Now, since $d(\sigma, \sigma') > n \Rightarrow L^n[\delta_{\sigma'}](\sigma) = 0$, we get that only (z, σ') such that $d(z, \sigma') = n$ are interesting for Eq. (A.16). Therefore, if $d(z, \sigma') = n$ and by using the induction step in Eq. (A.16), we have

$$L^{n+1}(\sigma, \sigma') = L[L^n[\delta_{\sigma'}]](\sigma) = \sum_{z, z_1: n-1} q(\sigma, z)q(\sigma, z_1) \dots q(z_{n-1}, \sigma'). \quad (\text{A.17})$$

□

Lemma 7. *Let $d(\sigma, \sigma') = k$. Then $L^k(\sigma, \sigma') > 0$.*

Proof. Lemma 6 gives us a representation for $L^k(\sigma, \sigma')$ when $d(\sigma, \sigma') = k$. Since all of the transition rates are non-negative,

$$L^k(\sigma, \sigma') = \sum_{z_1: k-1} q(\sigma, z_1) \dots q(z_{k-1}, \sigma') \geq q(\sigma, b_1) \dots q(b_{k-1}, \sigma') \geq 0$$

for all paths $b_{1:k-1}$ that connect σ and σ' . Since $d(\sigma, \sigma') = k$, there is a path such that the inequality above is strictly positive. □

Appendix B. Details about the coefficients of the relative entropy rate and the discrepancy term

Let L be a bounded operator, which allows us to represent the semigroup e^{Lt} via a power series expansion. We shall use the notation $L(\sigma, \sigma') := L[\delta'_\sigma](\sigma)$, with which we have

$$P_t(\sigma, \sigma') = e^{Lt} \delta_{\sigma'}(\sigma) = \sum_{k=0}^{\infty} \frac{L^k(\sigma, \sigma')}{k!} t^k. \quad (\text{B.1})$$

We assume that we can write an expansion for $Q_{\Delta t}$ too by representing each semigroup in Equation (3) and Equation (4) by its series and then multiplying out. By this process, we get

$$Q_{\Delta t}(\sigma, \sigma') = \sum_{k=0}^{\infty} \frac{L_Q^k(\sigma, \sigma')}{k!} \Delta t^k, \quad (\text{B.2})$$

where L_Q^k represents the terms of order k in the expansion of $Q_{\Delta t}$. For example, for the Lie splitting, $L_Q^0 = I$, $L_Q^1 = L$, $L_Q^2 = (L_1^2 + L_2^2 + 2L_1L_2)$. Note that the notation is picked for clarity and does not imply that L_Q is a generator of a Markov Process.

Lemma 8. *Under the assumptions of Lemma 2, if $A_{\text{Lie}}(A_{\text{Str}})$ is the highest order coefficient of the RER for the Lie (Strang) splitting, then*

$$\begin{aligned}
A_{\text{Lie}} &= \mathbb{E}_{\mu_{\text{Lie}}(\sigma)} \left[\sum_{x,y \in \Lambda} F_{\text{Lie}}(\sigma, \sigma^{x,y}) \right] = \sum_{\sigma} \mu_{\text{Lie}}(\sigma) \sum_{x,y \in \Lambda} F_{\text{Lie}}(\sigma, \sigma^{x,y}), \\
F_{\text{Lie}}(\sigma, \sigma') &:= C_{\text{Lie}}(\sigma, \sigma') M_L(\sigma, \sigma') - 2\text{Lie}_{\text{Lie}}^2[\delta_{\sigma'}](\sigma) (\text{arctanh}(M_{\text{Lie}}(\sigma, \sigma')) - M_{\text{Lie}}(\sigma, \sigma')), \\
M_{\text{Lie}}(\sigma, \sigma') &:= C_{\text{Lie}}(\sigma, \sigma') / (\text{Lie}_{\text{Lie}}^2[\delta_{\sigma'}](\sigma) + C_{\text{Lie}}(\sigma, \sigma'))
\end{aligned} \tag{B.3}$$

and, for the Strang splitting,

$$\begin{aligned}
A_{\text{Str}} &= \mathbb{E}_{\mu_{\text{Str}}(\sigma)} \left[\sum_{x,y,z \in \Lambda} F_{\text{Str}}(\sigma, \sigma^{x,y,z}) \right] = \sum_{\sigma} \mu_{\text{Str}}(\sigma) \sum_{x,y,z \in \Lambda} F_{\text{Str}}(\sigma, \sigma^{x,y,z}), \\
F_{\text{Str}}(\sigma, \sigma') &:= C_{\text{Str}}(\sigma, \sigma') M_{\text{Str}}(\sigma, \sigma') - 2L_{\text{Str}}^3[\delta_{\sigma'}](\sigma) (\text{arctanh}(M_{\text{Str}}(\sigma, \sigma')) - M_{\text{Str}}(\sigma, \sigma')), \\
M_{\text{Str}}(\sigma, \sigma') &:= C_{\text{Str}}(\sigma, \sigma') / (L_{\text{Str}}^3[\delta_{\sigma'}](\sigma) + C_{\text{Str}}(\sigma, \sigma')).
\end{aligned} \tag{B.4}$$

Proof. This is part of the proof of Theorem 2 in [12]. \square

Similarly, from the proof of Lemma 3, Section 5, we can write down the highest-order coefficient for the discrepancy.

Lemma 9. *Under the assumptions of Theorem 3, if $D_{\text{Lie}}(D_{\text{Str}})$ is the highest order coefficient of I for the Lie (Strang) splitting, then*

$$\begin{aligned}
D_{\text{Lie}} &= \sum_{\sigma} \mu_{\text{Lie}}(\sigma) \sum_{x \in \Lambda} \frac{q(\sigma, \sigma^x)}{q(\sigma^x, \sigma)} C_{\text{Lie}}(\sigma^x, \sigma) \\
&\quad + \sum_{x,y \in \Lambda} \mu_{\text{Lie}}(\sigma) L_{\text{Lie}}^2(\sigma, \sigma^{x,y}) \text{atanh}(M_{\text{Lie}}(\sigma^{x,y}, \sigma)).
\end{aligned} \tag{B.5}$$

and

$$\begin{aligned}
D_{\text{Str}} &= \sum_{\sigma} \mu_{\text{Str}}(\sigma) \left(\sum_{x \in \Lambda} \frac{L(\sigma, \sigma^x)}{L(\sigma^x, \sigma)} C_{\text{Str}}(\sigma^x, \sigma) + \sum_{x,y \in \Lambda} \frac{L^2(\sigma, \sigma^{x,y})}{L^2(\sigma^{x,y}, \sigma)} C_{\text{Str}}(\sigma^{x,y}, \sigma) \right. \\
&\quad \left. + \sum_{x,y,z \in \Lambda} L_{\text{Str}}^3(\sigma, \sigma^{x,y,z}) \frac{1}{3} \text{atanh}(M_{\text{Str}}(\sigma^{x,y,z}, \sigma)) \right).
\end{aligned} \tag{B.6}$$

Appendix C. Adsorption/Desorption Example

Here we include the setup for the adsorption/desorption example we simulated with the help of SPPARKS.

Let $\Lambda \subset \mathbb{Z}^2$ be a bounded, two-dimensional integer lattice. To every lattice site x corresponds a spin variable $\sigma(x)$, $\sigma(x) \in \Sigma = \{0, 1\}$, where $\sigma(x) = 0$ denotes that site x is empty and $\sigma(x) = 1$ that the site is occupied by some particle. The transition rates will correspond to single spin-flip Arrhenius dynamics. If we fix a state $\sigma \in S$ and a lattice site $x \in \Lambda$, then the transition rates q are defined by

$$q(\sigma, \sigma^x) = q(x, \sigma) = c_1(1 - \sigma(x)) + c_2\sigma(x)e^{-\beta U(x)}, \quad (\text{C.1})$$

$$U(x, \sigma) = J_0 \sum_{y \in \Omega_x} \sigma(y) + h. \quad (\text{C.2})$$

The constants, $c_1, c_2, -\beta, J_0, h$, can be tuned to generate different dynamics. σ^x is the resulting state after starting with σ and changing $\sigma(x)$ to $1 - \sigma(x)$. Ω_x represents the set of lattice sites that are neighbors of x . For this model, Ω_x will just be the nearest neighbors of x , like in Figure 1. This is the kind of spatial dependence on information that allows us to use parallel KMC.

The single spin-flip process, defined by the transition rates in (C.1), satisfies detailed balance and can be simulated exactly via Kinetic Monte Carlo.

Appendix D. Estimators of the EPR for a Diffusion Process

To show how the calculation of the estimators would change under a different model, we shall now demonstrate the case of a diffusion process. Let us assume that it is modeled by the set of transition rates

$$q(x, y, \sigma) = p(x, y)\sigma(x)(1 - \sigma(y)), \quad x, y \in \Lambda, \quad (\text{D.1})$$

for some state σ . At each time step, the system can swap the values between two lattice sites, x, y . $p(x, y)$ corresponds to some decaying potential that captures the distance a particle can travel. For instance, for nearest neighbor jumps, we would have $p(x, y) = 1/4$ if $|x - y| = 1$, and $p(x, y) = 0$ otherwise. Note that the transition rates q are zero if the origin site x is empty or if the target site y is occupied.

We focus on the case of computing the discrepancy term, I , for the Lie splitting with a splitting of the generator L into $L_1 + L_2$. Nevertheless, this example will also be instructive for the case of the relative entropy rate and other splittings.

Theorems 2 and 3 make no assumption on the underlying model. They do however use the notion of distance between states that the transition rates define (see discussion at the beginning of Section 5). For this model, two states σ, σ' , are one jump apart if there exist lattice sites x, y such that $\sigma' = \sigma^{x,y}$, and two jumps apart if there exist x, y, z, w such that $\sigma' = \sigma^{x,y,z,w}$. Therefore, after computing the corresponding commutator, $C_{\text{Lie}}(\sigma, \sigma') = [L_1, L_2]\delta_{\sigma'}(\sigma)$, and L_{Lie}^2 , we can write the exact formula for the highest order coefficient for the Lie splitting as

$$\begin{aligned}
D_{\text{Lie}} = & \sum_{\sigma} \mu_{\text{Lie}}(\sigma) \sum_{x,y \in \Lambda} \frac{q(\sigma, \sigma^{x,y})}{q(\sigma^{x,y}, \sigma)} C_{\text{Lie}}(\sigma^{x,y}, \sigma) \\
& + \sum_{x,y,z,w \in \Lambda} \mu_{\text{Lie}}(\sigma) L_{\text{Lie}}^2(\sigma, \sigma^{x,y,z,w}) \text{atanh}(M_{\text{Lie}}(\sigma^{x,y,z,w}, \sigma)).
\end{aligned} \tag{D.2}$$

Since the commutator C_{Lie} is zero for all choices of lattice sites but those at the boundaries between sub-lattices, $\partial\Lambda$, Equation (D.2) is actually

$$\begin{aligned}
D_{\text{Lie}} = & \sum_{\sigma} \mu_{\text{Lie}}(\sigma) \sum_{x,y \in \partial\Lambda} \frac{q(\sigma, \sigma^{x,y})}{q(\sigma^{x,y}, \sigma)} C_{\text{Lie}}(\sigma^{x,y}, \sigma) \\
& + \sum_{x,y,z,w \in \partial\Lambda} \mu_{\text{Lie}}(\sigma) L_{\text{Lie}}^2(\sigma, \sigma^{x,y,z,w}) \text{atanh}(M_{\text{Lie}}(\sigma^{x,y,z,w}, \sigma)).
\end{aligned} \tag{D.3}$$

Therefore, for nearest neighbor interactions in a square $N \times N$ lattice and $\sigma \sim \mu_{\text{Lie}}$, the coefficient in (D.3) has cost of computation $O(N^2)$. It should be noted though that estimating coefficient (D.3) is more of a diagnostic that does not have to be computed while simulating the large system.